Proceedings of the ASME 2014 33rd International Conference on Ocean, Offshore and Arctic Engineering
OMAE2014
June 8-13, 2014, San Francisco, CA

OMAE2014-24246

DYNAMIC RESPONSES OF A JACKET-TYPE OFFSHORE WIND TURBINE USING DECOUPLED AND COUPLED MODELS

Muk Chen Ong
MARINTEK
NO-7450, Trondheim, Norway
Email: muk.chen.ong@marintek.sintef.no

Erin E. Bachynski
CeSOS, AMOS
Norwegian University of Science and Technology
NO-7491 Trondheim, Norway
MARINTEK
NO-7450, Trondheim, Norway
Email: erin.bachynski@ntnu.no

Ole D. Økland
MARINTEK
NO-7450, Trondheim, Norway
Email: ole.okland@marintek.sintef.no

Elizabeth Passano
MARINTEK
NO-7450, Trondheim, Norway
Email: elizabeth.passano@marintek.sintef.no

ABSTRACT

This paper presents numerical studies of the dynamic responses of a jacket-type offshore wind turbine using both decoupled and coupled models. In the decoupled (hydroelastic) model, the wind load is included through time-dependent forces and moments at a single node on the top of the tower. The coupled model is a hydro-servo-aero-elastic representation of the system. The investigated structure is the OC4 (Offshore Code Comparison Collaboration Continuation) jacket foundation supporting the NREL 5-MW wind turbine in a water depth of 50m. Different operational wind and wave loadings at an offshore site with relatively high soil stiffness are investigated. The objective of this study is to evaluate the applicability of the computationally efficient linear decoupled model by comparing with the results obtained from the nonlinear coupled model. Good agreement was obtained in the eigen-frequency analysis, decay tests, and wave-only simulations. In order to obtain good results in the combined wind and wave simulations, two different strategies were applied in the decoupled model, which are 1) Wind loads obtained from the coupled model were applied directly as time-dependent point loads in the decoupled model; and 2) The thrust and torque from an isolated rotor model were used as wind loads on the decoupled model together with a linear aerodynamic damper. It was found that, by applying the thrust force from an isolated rotor model in combination with linear damping, reasonable agreement could be obtained between the decoupled and coupled models in combined wind and wave simulations.

Keywords: Offshore wind turbines, dynamic responses, jacket, bottom-fixed, random waves.

1 INTRODUCTION

Wind energy is a clean and efficient renewable energy source. Significant wind energy development is now taking place offshore. Based on cost and technological maturity, bottom-fixed support structures are adopted for most of the offshore wind turbine (OWT) designs in shallow/intermediate water regions. (Here the term OWT refers to the entire assembly of a wind turbine, which includes the rotor-nacelle assembly (RNA) and a support structure.) OWTs are subject to dynamic environmental loads from the air, water and soil. In order to ensure structural safety of all of the components, accurate and detailed dynamic analysis of the complex OWT behavior is required.

Integrated numerical tools, such as FAST, HAWC2 (Horizontal Axis Wind turbine simulation Code), Bladed, Flex5, and SIMO-RIFLEX-AeroDyn, have been developed by several research institutes for performing dynamic analyses. In the present study, SIMO-RIFLEX-AeroDyn is adopted for the dynamic coupled analyses.

SIMO-RIFLEX is a nonlinear time-domain numerical program developed by MARINTEK. The finite element formulation employed in SIMO-RIFLEX can handle finite displacement and rotations. Coupled analysis can be performed using SIMO-RIFLEX, where one or more rigid body floating structures are integrated with a dynamic mode of the mooring, riser systems and arbitrary coupling forces in the time domain; see Ormberg (1997). For wind turbine applications, the structure (including the rotor components) is modeled in SIMO-RIFLEX, while AeroDyn (Moriarty and Hansen, 2005) provides the forces and moments on the turbine blades based on Blade Element/Momentum (BEM) or Generalized Dynamic Wake (GDW), including dynamic stall, tower shadow, and skewed inflow correction. The dynamic finite element solution is obtained from SIMO-RIFLEX, which passes displacement/velocity information to AeroDyn and receives loads from AeroDyn at each time step. The combination of SIMO-RIFLEX and AeroDyn, which forms SIMO-RIFLEX-AeroDyn (SRA), provides a stable nonlinear finite element solver, sophisticated hydrodynamics, well-tested aerodynamics, and control logic. The detailed documentation of SRA can be referred to Ormberg and Bachynski (2012).

Another MARINTEK in-house numerical code developed for structural analysis, NIRWANA, is used to perform decoupled analyses in the present study. NIRWANA is a linear time-domain numerical program based on a finite element method. It was previously developed for studying wave-induced structural loads and responses of bottom-fixed structures, e.g. offshore jacket platforms (see Karunakaran (2001)), in both regular and random waves. This numerical tool is very computationally efficient, which is a useful characteristic when studying structures subjected to a wide range of environmental conditions.

The objective of this study is to evaluate the applicability of the computationally efficient linear decoupled model by comparing with the results obtained from the nonlinear coupled model. The OC4 5-MW jacket-type OWT is chosen as the reference structure. The OWT is located at an offshore site with 50m water depth and relatively high soil stiffness. Wave loads are calculated according to different operational conditions of the wind turbine (i.e. for wind speeds within the cut-in and cut-off conditions). Comparisons between the linear decoupled model and non-linear coupled model are made for an eigen-frequency analysis, a decay test, and for dynamic simulations with wave-only excitation and combined wind-wave conditions.

2 DESCRIPTION OF THE DYNAMIC MODELS

The OC4 5-MW jacket-type OWT is selected for this case study. The NREL 5-MW offshore baseline turbine defined by Jonkman et al. (2009) is supported by the UpWind project reference jacket model developed by Vemula et al. (2010), and then further used by Vorpahl et al. (2011) for the OC4 benchmark exercise. As shown in Figure 1, the support structure consists of a jacket substructure, a transition piece, and a tower. The four legs of the jacket are supported by piles which are clamped at the seabed (50m water depth). The legs are stiffened by 4 levels of X-braces. The jacket and the tower are connected through a rigid transition piece. The elevation of the entire support structure above the still water level is 88.15m, and the hub height is 90.55m. In the present study, the OWT is assumed to be located at an offshore site with relatively high soil stiffness. Thus, the substructure is assumed to be rigidly fixed to the sea bed. Furthermore, the effect of marine growth is not considered in the present study. The detailed dimensions and material properties of the support structure can be referred to Vorpahl et al. (2011).

The OWT model built in NIRWANA is linear and hydroelastic with a decoupled model for the turbine, whereas a hydro-servo-aero-elastic non-linear model is built in SIMO-RIFLEX-AeroDyn, see Figure 1. The support structures in both the NIRWANA and SRA models have the same discretization: the same number of elements and nodes, see Table 7, and the same element properties.

The hydrodynamic loads due to linear, long-crested random waves were considered in the present study. The JONSWAP spectrum was applied for generation of the random waves. Time histories of the sea surface elevation, water particle velocity, and acceleration were generated in SIMO, with frequency resolution $\Delta\omega = 0.002$, using a Cooley-Tukey Fourier transform algorithm. The same wave histories were applied in NIRWANA. The hydrodynamic forces on the OWT were calculated using Morison's equation. In NIRWANA, Wheeler stretching (Wheeler, 1970) was applied in the wave simulation in order to calculate the wave induced velocities and accelerations at the correct vertical elevations along the supporting structure of the OWT. In SRA, constant wave particle velocities were applied above the mean water level.

Wave and wind conditions are correlated because waves in the ocean are mainly wind-generated. A wind-wave model proposed by Ong et al. (2013) was adopted in the present study. For a given hub height mean wind speed (V_{hub}), the sea-state can be defined based on semi-analytical functions. Only linear wind-generated waves were considered in the present study. When the wind-wave data is unavailable in a shallow water region, this model can provide an estimation of the sea state based on the deep water wind-wave condition.

The cut-in and cut-off wind speeds of the NREL 5 MW wind turbine are 3 m/s and 25 m/s, respectively. Table 1 shows the wind-generated significant wave height (H_s) and peak period (T_p), in the 50m water depth corresponding to several values of V_{hub} within the range of operational conditions of the NREL 5 MW turbine. These wave conditions are then applied for calculations of the hydrodynamic loadings on the OC4 OWT.

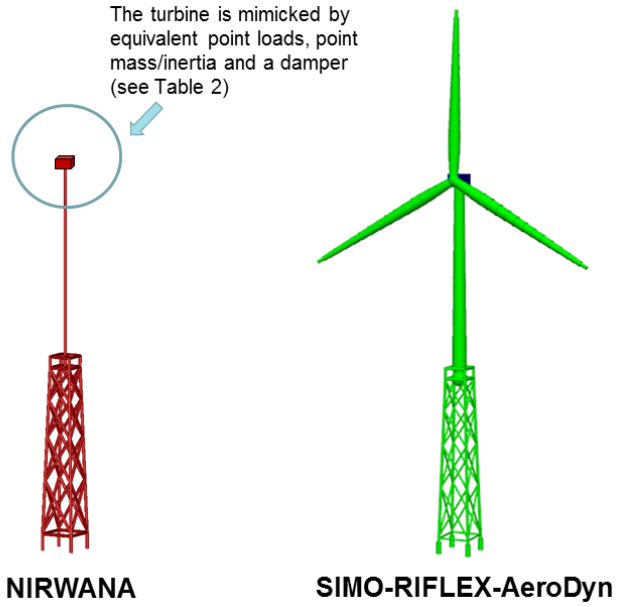

Figure 1: Schematic diagrams of both the NIRWANA and SIMO-RIFLEX-AeroDyn models. Note that the airfoil shapes are included in the SRA analysis, but not in the schematics.

Table 1: Environmental conditions (ECs)

Condition	V_{hub} (m/s)	Linear Random Waves (50 m water depth)	
		H_s (m)	T_p (s)
EC 1	7.0	0.63	4.03
EC 2	11.4	1.69	6.55
EC 3	15.0	2.85	8.27
EC 4	20.0	4.67	10.47

3 RESULTS AND DISCUSSION

In order to evaluate the applicability of the computationally efficient linear decoupled model, a sequence of comparisons has been carried out in a step by step manner, as summarized in Table 2. An eigen-frequency analysis, decay test, simulations with only wave excitation, and combined wind-and wave simulations were considered. Two decoupling methods were applied for the combined wind-wave simulations: decoupling method 1 (i.e., wind loads are modeled by 6 component internal loads from the nonlinear coupled model) and decoupled method 2 (i.e., wind loads are modeled by selected forces and moments from the isolated rotor plus an aerodynamic linear damper).

In the wave-only and wind-wave simulations, load comparisons are presented for a limited number of structural components. Figure 2 shows the selected locations (tower top, tower base, and Element 1) for comparisons between the results of the NIRWANA model (linear, decoupled) and the SRA model (nonlinear, coupled) in terms of the axial force in Element 1, the tower base moment and the displacement of the tower top in the x-direction. Element 1 is the bottom component of one of the downwind legs. The global coordinate system, which is fixed at the tower top, is defined as shown in Figure 3.

Table 2: Summary of comparison cases

Case	Model / Purpose	**NIRWANA**	**SRA**
Eigen-frequency analysis	Natural frequencies	*point mass/inertia	no wind, parked rotor
Decay test	Structural damping	*point mass/inertia	no wind, parked rotor
Wave-only	Hydrodynamic loading	*point mass/inertia	no wind, parked rotor
Wind-wave	Combined loads	1) Point loads from the SRA full model	BEM (EC 1) and GDW (EC 2-4) aerodynamic loads
		2) Point loads from an isolated rotor, *point mass/inertia and a linear damper	

**Jacket, tower +*

**Full model +*

**Point mass/inertia includes the contribution from the nacelle, hubs and blades, i.e., a single point mass/inertia for the Rotor-Nacelle assembly (RNA).*

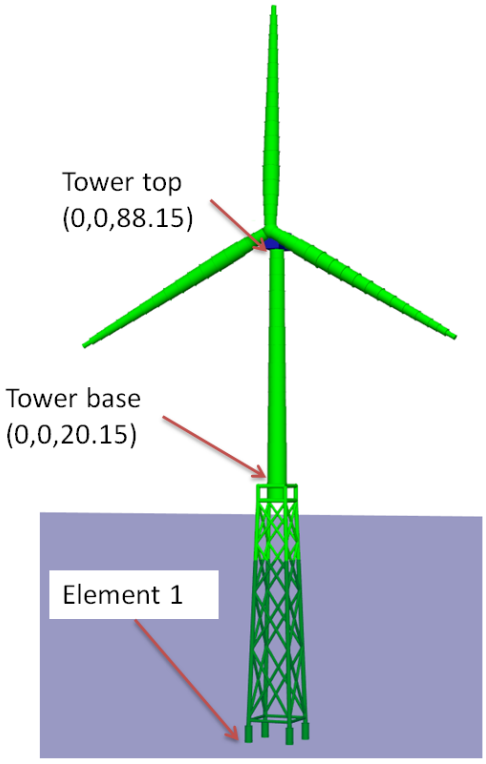

Figure 2: Selected locations, i.e. tower top, tower base, and Element 1, for comparisons between the decoupled and coupled models.

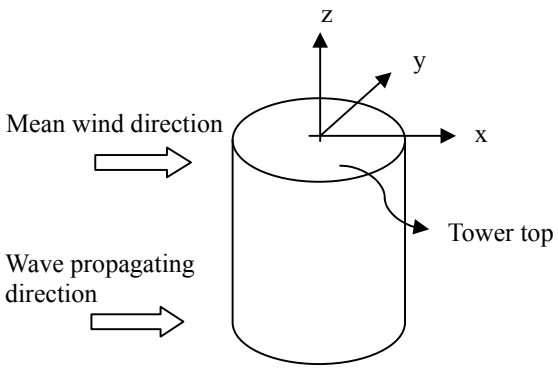

Figure 3: The global coordinate system at the tower top.

3.1 Eigen-Frequency Analysis

Eigen-frequency analyses were carried out for the NIRWANA (decoupled) and SRA (coupled) models. In the NIRWANA model, the turbine was modeled as a point mass/inertia with its corresponding mass moments of inertia (see the detailed description of the turbine in Jonkman et al. (2009)). Table 3 shows the results of the eigen-frequency analyses for the NIRWANA and SRA models together with the reported OC4 results from Popko et al. (2012). The natural periods for the 1st fore-aft mode (in the x-z plane), 1st side-to-side mode (in the y-z plane), 2nd fore-aft, and 2nd side-to-side are tabulated. The NIRWANA model generally gives slightly shorter natural periods for 1st fore-aft mode and 1st side-to-side mode as compared to that of the SRA model. This is physically sound because the whole turbine with flexible blades is modeled in the coupled model, while there is only a point mass/inertia representation in the decoupled model. Therefore, the nonlinear coupled model will behave slightly "softer" structurally than the linear decoupled model. This can also be seen in the natural periods of the SRA* model with a rigid RNA, which are shorter than the natural periods of the SRA model. The results obtained from the NIRWANA model lie within the published results summarized by Popko et al. (2012). The predicted 1st fore-aft and 1st side-to-side natural periods of the SRA model are slightly (<1.2 %) higher than the upper bounds of the published results. For the 2nd fore-aft mode and 2nd side-to-side mode, the predictions by SRA are in good agreement with the published results. Overall, the present predictions by the NIRWANA and SRA model are in reasonable agreement with the published results.

The SRA model is also able to reproduce rotor and blade bending frequencies in good agreement with Popko et al. (2012).

Table 3: Eigen-frequency analysis results. SRA* results are for the SRA model with rigid RNA.

	Natural Periods (s)			
	NIRWANA	SRA	SRA*	Popko et al. (2012)
1st Fore-Aft	3.234	3.346	3.333	3.12-3.31
1st Side-to-Side	3.215	3.331	3.315	3.13-3.30
2nd Fore-Aft	0.891	0.840	0.884	0.80-0.91
2nd Side-to-Side	0.873	0.823	0.866	0.74-0.90

3.2 Decay Test

After confirming the natural frequencies of the models, a decay test was performed to ensure that the NIRWANA and SRA models have similar structural damping behavior. According to Vorpahl et al. (2011), all modes of the support structure (without RNA) should have 1% critical damping. In both NIRWANA and SRA, the structural damping is modeled by stiffness-proportional Rayleigh damping. The structural damping therefore depends on frequency. The stiffness-

proportional damping coefficients were chosen to give reasonable damping ratios for the first two structural modes, but it is impossible to obtain 1% damping in both modes.

Figure 4 shows the configuration of the decay test, which was performed in still water with no wind. The structure was first brought to static equilibrium under a 1000 kN point load on the hub in the x-direction; the load was subsequently removed in order to examine the decay.

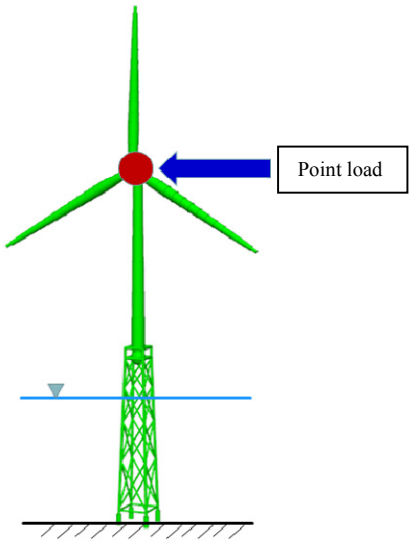

Figure 4: Configuration of the decay test.

Figure 5 shows that the structural damping behavior of the NIRWANA model behaves similarly to that of the SRA model. For the 1st fore-aft mode, the critical structural damping ratios for the NIRWANA model and the SRA model are 0.42% and 0.45%, respectively.

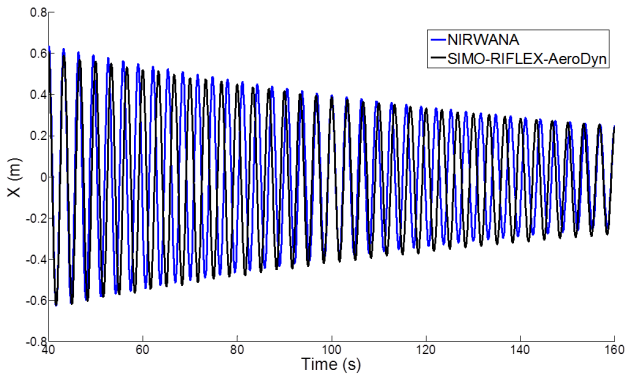

Figure 5: Time-history of tower top displacements in the x-direction for the NIRWANA and SRA models (decay test).

3.3 Wave-Only Simulations

Dynamic simulations with only wave excitation were performed using the NIRWANA model and the SRA model for the EC 3 and EC 4 wave conditions (see Table 1). In the NIRWANA model, the turbine was modeled as a point mass/inertia with mass and inertia corresponding to the RNA of the NREL 5 MW wind turbine. In the SRA model, the rotor was parked and no wind forces were applied. The time-series of the axial force in Element 1 (see Figure 2) for EC4 is shown in Figure 6. The NIRWANA model and the SRA model give similar time-series results.

Figure 7 shows the spectrum of the axial force in Element 1 for EC4. The majority of the force variation occurs in the wave frequency range, where there is good agreement between the two models. An additional, smaller, spectral peak is visible at the 1st fore-aft natural frequency. The SRA model gives higher excitation at the 1st fore-aft natural period compared to the NIRWANA model. There is some wave forcing at this frequency due to "3ω" effects from the viscous drag on the jacket legs. High-frequency forcing may also be present due to phase differences in the inertial forces on different components. The two programs have slightly different implementations of hydrodynamic loading on the elements. Since the structure is lightly damped, small load differences at the natural frequency can result in larger differences in the response. Table 4 summarizes the mean values and the standard deviations of the axial force in Element 1 for EC3 and EC4. Despite the differences in the spectra near the first fore-aft period, the statistical results from the NIRWANA and SRA models are generally in good agreement.

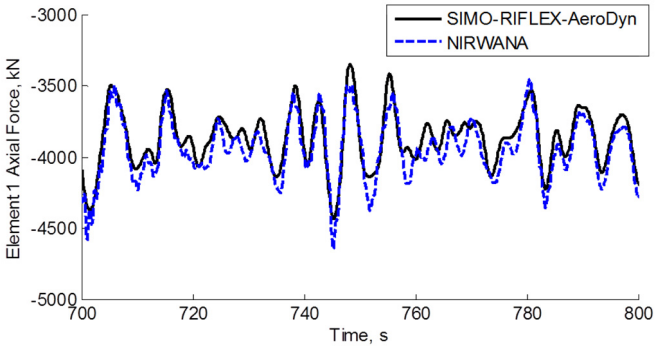

Figure 6: Time-series of the axial force in Element 1 for EC4.

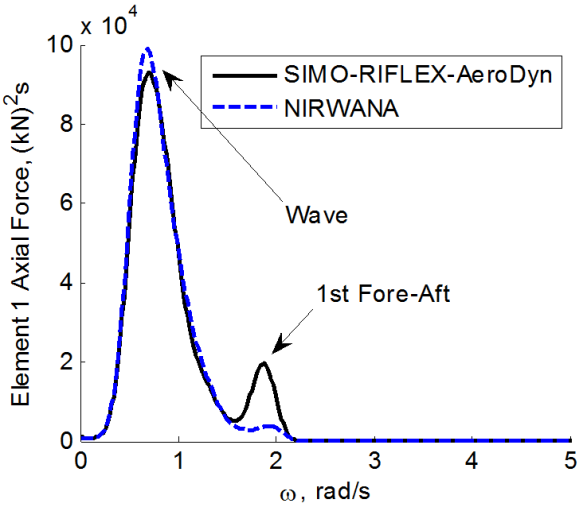

Figure 7: Spectrum of the axial force in Element 1 for EC4.

Table 4: Summary of the mean values and the standard deviations of the axial force in Element 1 for EC3 and EC4.

Element 1 Axial Force				
	Mean (kN)		Standard Deviation (kN)	
	NIRWANA	SRA	NIRWANA	SRA
EC 3	-3.93×10^3	-3.86×10^3	1.67×10^2	1.86×10^2
EC 4	-3.93×10^3	-3.87×10^3	2.48×10^2	2.52×10^2

3.4 Decoupling Method 1

Next, combined wind and wave loads were considered. In the first approach, internal loads obtained from the coupled model were applied directly as time-dependent point loads in the decoupled model, as in Figure 8. The point mass and the mass moments of inertia were not included in this decoupled model. Gao et al. (2010) showed that this decoupled method can be used with good accuracy provided that there are not any conflicts in the forcing and response frequencies.

Table 5 shows the summary of the NIRWANA and SRA results of the axial force in Element 1 for EC1 to EC4 using decoupling method 1. Although the mean values are in good agreement, the decoupled NIRWANA model exhibits larger standard deviation.

Since the turbine mass was not included in decoupled model 1, the response characteristics of the support structure are altered. The updated natural periods for the 1st fore-aft mode and the 1st side-to-side mode for the decoupled model 1 are 1.376s and 0.651s, respectively. These periods lie within the range of the first and second blade bending modes (0.51s - 1.66s for flapwise and edgewise pitch and yaw, and collective flap). As a result, the internal loads at the tower top include components at the blade vibration frequencies. Larger dynamic responses are therefore observed in the decoupled model 1, as shown in Figure 9, where the spectra of the axial force in Element 1 for both the decoupled model 1 and the SRA model for EC2 are shown. The wind, wave, structural and wind turbine excitation frequencies are identified.

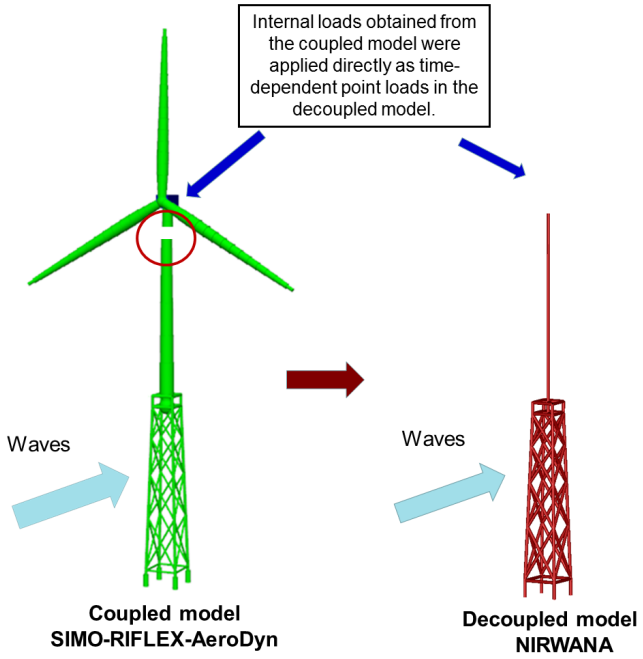

Figure 8: The configuration of Decoupling Method 1.

Table 5: Summary of the NIRWANA and SRA results for the axial force in Element 1 for EC1 to EC4, combined wind-wave excitation, decoupling method 1.

Element 1 Axial Force				
	Mean (kN)		Standard Deviation (kN)	
	NIRWANA	SRA	NIRWANA	SRA
EC 1	-5.57×10^3	-5.68×10^3	7.45×10^2	4.35×10^2
EC 2	-7.23×10^3	-7.35×10^3	1.19×10^3	5.50×10^2
EC 3	-6.11×10^3	-6.33×10^3	1.35×10^3	5.38×10^2
EC 4	-5.47×10^3	-5.84×10^3	1.81×10^3	6.08×10^2

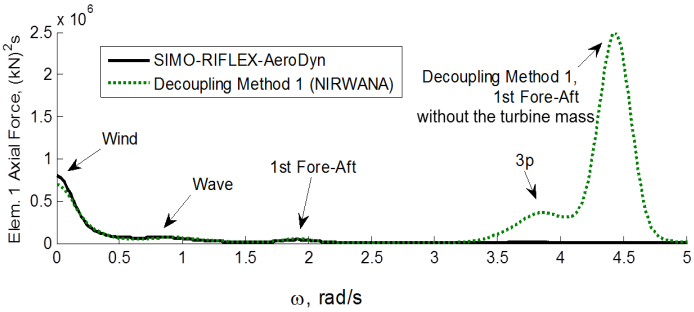

Figure 9: Spectra of the axial force in Element 1 for both the decoupled model 1 and the SRA model for EC 2.

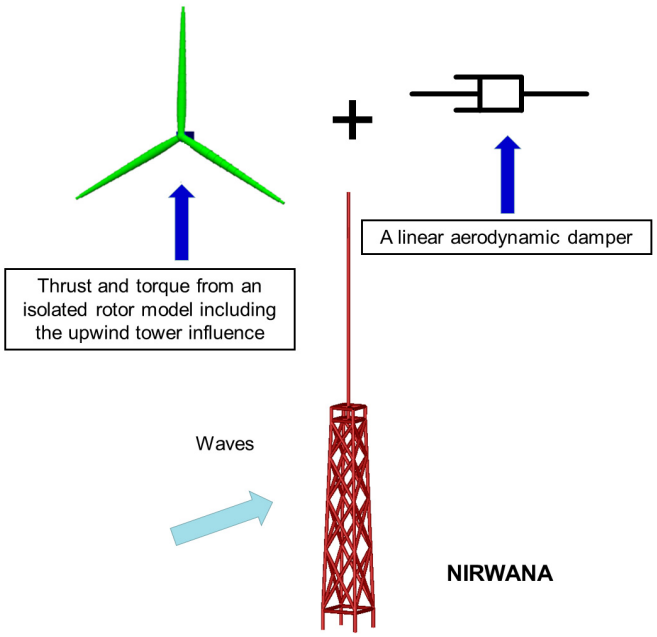

Figure 10: Configuration of decoupling method 2.

3.5 Decoupling Method 2

Because the dynamic responses were significantly over-predicted by decoupling method 1 (see Table 5 and Figure 9), an improved decoupling method was suggested to address these shortcomings. In the decoupling method 2 (NIRWANA), the thrust and torque from an isolated SRA rotor model including the upwind tower influence were used as wind loads on the decoupled model 2. In addition, a linear damper was introduced to account for the aerodynamic damping. The force on the hub due to the linear damper is modeled as $F_{aerodamping} = -CU_x$, where C is the aerodynamic damping coefficient and U_x is the structural velocity at the tower top in the x-direction. C is generally taken as dF_T/dV_{hub}, where F_T is the rotor thrust force, calculated for steady wind speeds without considering the effect of the control system. The details of this linear aerodynamic damping estimation can be referred to Salzman and Tempel (2005) and Bachynski (2014). Figure 10 shows the configuration of the decoupling method 2.

The dynamic responses of the decoupled model 2 were then compared with those of the coupled model for EC1-EC4. Figure 11 shows the time-series plots of the axial force in Element 1, the tower base moment about the y-axis, and the displacement of the tower top in the x-direction for EC 2 (i.e. the environmental condition with the largest thrust). The results obtained from the decoupled model 2 (NIRWANA) agree reasonably well with the results from the coupled model (SRA).

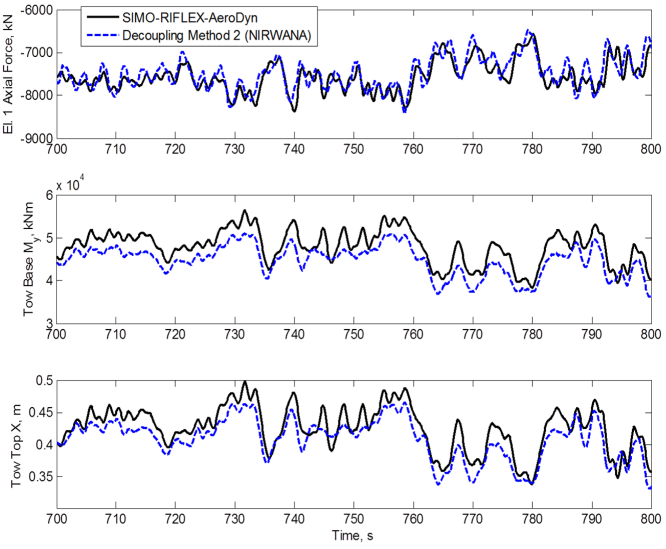

Figure 11: Time-series plots of the axial force in Element 1, the tower base moment, and the displacement of the tower top in x-direction for EC2, combined wind and waves.

Figures 12 and 13 show the spectral plots of the axial force in Element 1, the tower base moment, and the displacement of the tower top in x-direction for EC2 (with the largest thrust) and EC4 (with the largest wave), highlighting the components at the wind, wave, structural, and wind turbine excitation (such as blade passing) frequencies. In Figure 12, the decoupled model 2 (NIRWANA) gives slightly lower response at the wind frequency as compared to the SRA model. This might be attributed to the limited accuracy in modeling the actual aerodynamic damping by using the aforementioned linear damper. In Figure 13, the decoupled method 2 gives larger dynamic responses than the SRA model at the 1st fore-aft natural frequency. Generally, the spectral analyses show that decoupled model 2 and the SRA model are in reasonable agreement.

Table 6 shows the mean values and the standard deviations of the axial force in Element 1 for EC2 and EC4. Statistically, the decoupled model 2 and the coupled model are in good agreement: the mean values differ by less than 6 %, and the standard deviations are within 8 %.

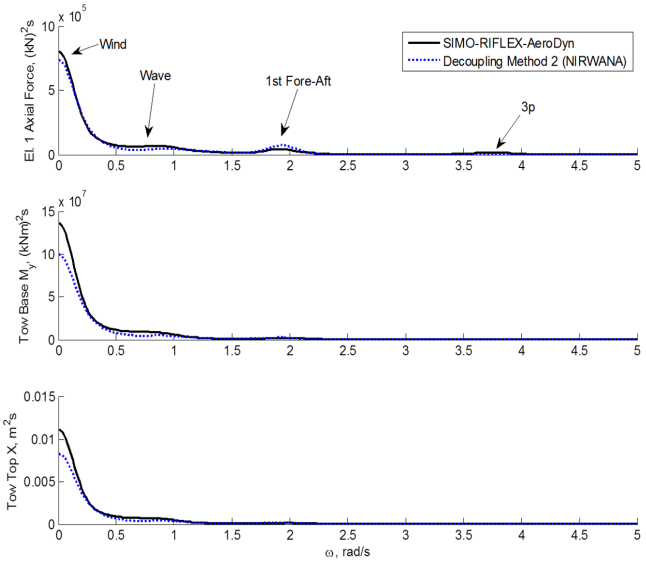

Figure 12: Spectral plots of the axial force in Element 1, the tower base bending moment, and the displacement of the tower top in x-direction for EC2, combined wind and waves.

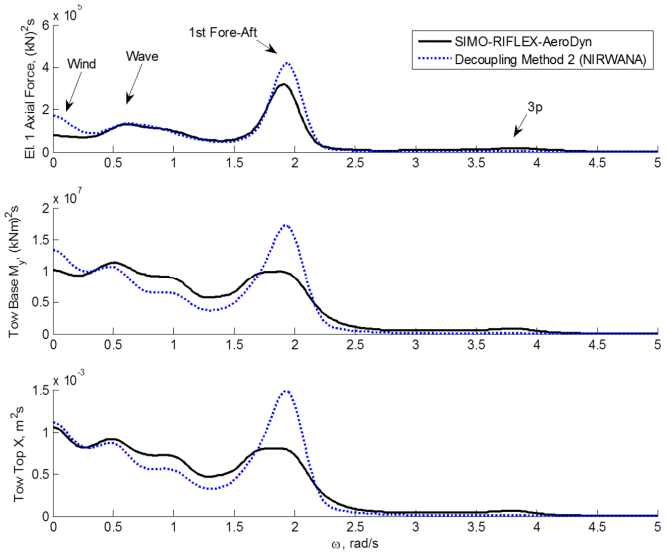

Figure 13: Spectral plots of the axial force in Element 1, the tower base moment, and the displacement of the tower top in x-direction for EC4, combined wind and waves.

Table 6: Mean values and standard deviations of the axial force in Element 1 for EC2 and EC4, wind-wave simulations, decoupling method 2.

Element 1 Axial Force				
	Mean (kN)		Standard Deviation (kN)	
	NIRWANA	SRA	NIRWANA	SRA
EC 2	-7.26×10^{3}	-7.35×10^{3}	5.10×10^{2}	5.50×10^{2}
EC 4	-5.52×10^{3}	-5.84×10^{3}	5.65×10^{2}	6.08×10^{2}

In order to investigate the large discrepancy between the decoupled model 2 (NIRWANA) and the SRA model at the 1st fore-aft natural frequency as shown in Figure 13, a new decoupled model 2 using SIMO-RIFLEX was built. Figure 14 shows the spectral comparisons between the SRA model, the decoupled model 2 (NIRWANA), and the decoupled model 2 (SIMO-RIFLEX) in terms of the axial force in Element 1, the tower base moments about y direction, and the displacement at tower top in x direction under EC4. The decoupled model 2 (NIRWANA) and the decoupled model 2 (SIMO-RIFLEX) are in good agreement. The difference in response at the first fore-aft frequency lies between the coupled and the decoupled models, and not between the linear and the non-linear models.

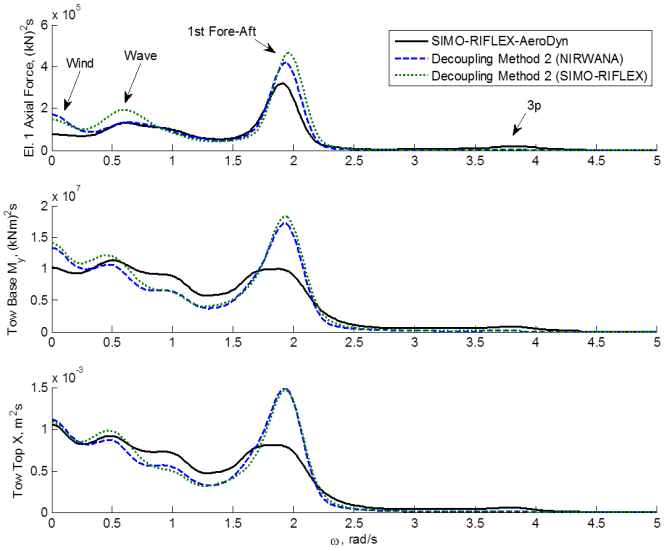

Figure 14: Spectral plots of the axial force in Element 1, the tower base moment and the displacement of the tower top in x-direction for EC4.

3.6 Computational Efficiency

Using the two versions of decoupled model 2 compared in Figure 14, the computational efficiency of the linear and non-linear models could be compared. The linear decoupled model (NIRWANA) and the non-linear decoupled model (SIMO-RIFLEX) were simulated on a computer with Intel i7CPU 1.73GHz and 16GB RAM, with identical simulation inputs. As shown in Table 7, the linear simulation was around 8 times faster than the non-linear simulation. It should be noted that the non-linear simulation takes significantly longer when the rotor is included. If the nonlinear response of the investigated support structure is not significant, i.e., for a structure with rather small deformation, a linear model (NIRWANA) could be a good engineering tool for performing dynamic analyses, particularly for long-term fatigue studies.

Table 7: Computational time comparison for linear and non-linear models, decoupling method 2 (not including wind load generation).

Nodes	74	
Elements	137	
Time steps	8192	
Actual simulation time (s)	**NIRWANA**	**SRA**
	8.2	64.5

CONCLUSIONS

Numerical studies of dynamic responses of the OC4 jacket-type offshore wind turbine (OWT) using both linear decoupled and nonlinear coupled models have been carried out. Comparisons between the linear decoupled models and non-linear coupled model were evaluated through performing eigen-frequency analyses, a decay test, and dynamic simulations with only wave excitation and combined wind-wave conditions within the operational conditions of the OWT. The main results are summarized as follows:

- NIRWANA and SRA models were in good agreement with published eigen-frequency analyses of the structure.
- Wave-only simulations showed good agreement between the coupled and decoupled models in the wave frequency, with some differences at the first bending natural frequency.
- Decoupling method 1 (direct application of internal loads from a coupled simulation) gives poor results for this structure.
- Decoupling method 2 (thrust force from an isolated rotor model in combination with a linear aerodynamic damping) gives reasonable mean and standard-deviation results.
- The differences in the results between the decoupled model 2 and the coupled model are primarily due to the decoupling, not non-linearity.

This study considers a single jacket OWT in a limited number of environmental conditions. In order to fully evaluate the applicability of linear decoupled models, further work should address other structures, additional load cases, and comparisons with model testing and full-scale measurements. Nevertheless, the present study should be useful for engineering assessments related to the global dynamic analysis of jacket-type offshore wind turbines.

ACKNOWLEDGEMENT

This work has been supported by NOWITECH (Norwegian Research Centre for Offshore Wind Technology) which is co-funded by the Research Council of Norway, industrial companies and participating research organizations (http://www.nowitech.no). The second author is supported by CeSOS and by Statoil through an MIT-NTNU Gemini cooperative research project. The authors are grateful to Dr. Zhen Gao from CeSOS for valuable discussions.

REFERENCES

Bachynski, E.E., 2014. Design and Dynamic Analysis of Tension Leg Platform Wind Turbines. Ph.D. Thesis, Department of Marine Technology, NTNU, Norway.

Gao, Z., Moan, T. and Amdahl, J., 2010. Dynamic Analysis of Offshore Fixed Wind Turbines under Wind and Wave Loads using Alternative Computer Codes. TORQUE2010: The Science of Making Torque from Wind.

Jonkman, J.M. and Buhl, M.L.J., 2005. FAST User's Guide. National Renewable Energy Laboratory (NREL) , USA.

Jonkman, J.M., Butterfield, S., Musial, W. and Scott, G., 2009. Definition of a 5-MW Reference Wind Turbine for Offshore System Development. Tech. rep.NREL/TP-500-38060, National Renewable Energy Laboratory (NREL), USA.

Karunakaran, D., Haver, S., Bærheim, M., and Spidsøe, N., 2001. Dynamic behaviour of the Kvitebjørn jacket in the North Sea. Proceedings of the 20th International Conference on Offshore Mechanics and Arctic Engineering, OMAE01/OFT-1184, Rio de Janeiro, Brazil.

Moriarty, P.J. and Hansen, A.C., 2005. AeroDyn Theory Manual. Tech. rep. NREL/TP-500-36681.

Ong, M.C., Li, H., Leira, B.J., and Myrhaug, D., 2013. Dynamic analysis of offshore monopile wind turbine including the effects of wind-wave loading and soil properties. Proceedings of 32nd International Conference on Ocean, Offshore and Arctic Engineering, OMAE2013-10527, Nantes, France.

Ormberg, H., and Bachynski, E.E., 2012. Global analysis of floating wind turbines: code development, model sensitivity and benchmark study. Proceedings of the 22nd International Ocean and Polar Engineering Conference, Rhodes, Greece, Vol. 1, pp. 366-373.

Ormberg, H., Fylling, I., Larsen, K., and Sødahl, N., 1997. Coupled analysis of vessels motions and mooring and riser system dynamics. Proceedings of the 16th International Conference on Offshore Mechanics and Arctic Engineering, Yokohama, Japan.

Popko, W., Jonkman, J., Robertson, A., Larsen, T.J., Saetertro, K., Okstad, K.M., Nichols, J., Nygaard, T.A., Shi, W., Park, H.C., Gao, Z., Manolas, D., Basquez-Rojas, A., Dubois, J., Kohlmeier, M., Yde, A., Kaufer, D., de Ruiter, M.J., Peeringa, J., Kim, K. and von Waaden, H., 2012. Offshore Code Comparison Collaboration Continuation (OC4), phase I - results of coupled simulation of offshore wind turbine with jacket support structure. Proceedings of the 22nd International Offshore and Polar Engineering Conference, Rhodes, Greece, Vol. 1, pp. 337-346.

Salzmann, D. J. C., and van der Tempel, J., 2005. Aerodynamic damping in the design of support structures for offshore wind turbines. Proceedings of the Offshore Wind Energy Conference, Copenhagen, Denmark.

Vemula, N. K., DeVries, W., Fischer, T., Cordle, A., and Schmidt, B., 2010. Design solution for the UpWind reference offshore support structure. Upwind Deliverable D4.2.6 (WP4: Offshore Foundations and Support Structures), Rambøll Wind Energy.

Vorpahl, F., Kaufer, D., and Popko, W., 2011. Description of a basic Model of the "UpWind Reference Jacket" for code comparison in the OC4 project under IEA wind annex 30. Technical report, Fraunhofer Institute for Wind Energy and Energy System Technology IWES.

Wheeler, J.D., 1970. Method for calculating forces produced by irregular waves. Journal of Petroleum Technology, 249, 359-367.